

Chapter 5

High Precision Density Studies near the Smectic A – Nematic Tricritical Point

5.1 Introduction

The nematic (N) to smectic A (Sm A) phase transition is characterised by the onset of a density wave with a wavevector $q_o = 2\pi/d$, where d is the layer spacing. This mass density wave with wavevector along the z -axis, i.e., along the director, is well described by

$$\rho(r) = \rho_o \left[1 + \text{Re} \left(|\psi| e^{i(q_o z + \phi)} \right) \right] \quad (5.1)$$

where, ρ_o is the average density, ϕ is the phase factor which fixes the position of the layers, $|\psi|$ is the amplitude of the density wave which is a measure of the strength of smectic order. This smectic order is fully specified by a complex number $\psi = |\psi| e^{i\phi}$ where, $\phi = q_o u$, u is the displacement of the layers in the z -direction away from their equilibrium position. Transition between the nematic and smectic A phases can be either first order or second order with a tricritical point separating these two different behaviours.

Experiments have shown¹ that for a sufficiently large temperature range of the nematic phase, the nematic order is saturated and the transition is second order. When this range is reduced, the coupling between nematic and smectic order parameters increases and drives the N-Sm A transition from second order to first order. McMillan² made a self-consistent mean field calculation by incorporating the coupling between orientational and smectic ordering. According to this theory the appearance of the tricritical point is controlled by a parameter $r = T_{AN}/T_{NI}=0.87$, where T_{AN} and T_{NI} are the N-Sm A and N-isotropic transition temperatures respectively.

de Gennes³ argued that owing to the complex nature of ψ , the N-Sm A transition should belong to the same universality class ($d=3$, $n=2$ isotropic) as the normal-superfluid transition and should exhibit **3D** XY critical behaviour. There have been several theories⁴⁻⁸ based on this model which have attempted to describe the observed N-Sm A critical behaviour, including the anisotropic correlation lengths along ($\xi_{\parallel} = \xi_{\parallel}^0 |t|^{-\nu_{\parallel}}$) and transverse ($\xi_{\perp} = \xi_{\perp}^0 |t|^{-\nu_{\perp}}$) to the layer-normal, as well as the susceptibility ($\chi = \chi_0 |t|^{-\gamma}$), and specific heat at constant pressure ($C_p = A |t|^{-\alpha}$). Here $t = (T - T_{AN})/T_{AN}$. These theories place the N-Sm A transition either in the inverted 3D XY universality class⁵ (identical to the **3D** XY class except that the temperature axis is inverted) or in an anisotropic class. For the 3D XY universality class the predicted critical exponents⁹ are $\nu_{\parallel} = \nu_{\perp} = \nu_{XY} = 0.66$, $\gamma = 1.32$ and $\alpha = -.007$. For the anisotropic class, gauge transformation theory⁶ suggests extreme anisotropy, viz., $\nu_{\parallel} = 2\nu_{\perp}$ while dislocation mediated melting theory⁷ predicts $\nu_{\parallel} = 0.83$, $\nu_{\perp} = 0.53$. On the experimental side, N-Sm A transition has been studied by several experimental techniques^{1,8,10} including X-ray diffraction, light scattering and heat capacity. Measurements of the intensity and the width of the X-ray scattering yield the susceptibility (χ) and the correlation lengths (ξ) respectively. Light scattering which also gives the divergence of the elastic constants, can be used to measure ξ and has been found to give values in excellent agreement with those obtained from X-ray measurements. Two notable factors observed in experiments, in disagreement with any of the theories are (1) non-universal values for all the exponents ($0.57 \leq \nu_{\parallel} \leq 0.83$, $0.39 \leq \nu_{\perp} \leq 0.68$, $0 \leq \alpha \leq 0.5$ & $1.1 \leq \gamma \leq 1.53$), (2) small but finite anisotropy in correlation length exponents ($\nu_{\parallel} - \nu_{\perp} \sim 0.13$). Interestingly all the

materials satisfy the anisotropic hyperscaling relation, $\nu_{\parallel} + 2\nu_{\perp} + a = 2$ to within the experimental limits. Recent high resolution calorimetric measurements¹¹ on a few materials with large nematic temperature ranges have yielded a values exactly equal to that predicted by the 3D XY model. X-ray experiments¹² on another compound with a large range of the nematic phase has led to an interesting explanation for the observed anisotropy in ν_{\parallel} , ν_{\perp} values; the splay elastic constant is suggested to alter the critical behaviour of ξ_{\perp} , thus influencing the value of ν_{\perp} . In summary, therefore, the N-Sm A transition which is the most extensively studied transition in liquid crystals remains a major unsolved problem in condensed matter physics.

As pointed earlier a 3D XY value for a is seen in compounds which had a large temperature range for nematic phase.¹¹ But with an increase in $r (= T_{NA}/T_{NI})$ or with a decrease in the nematic phase temperature range, the exponent a , characterising the critical heat capacity departed from the 3D-XY value, through intermediate positive values, to values close to 0.50, a tricritical exponent ($\alpha=0.5$ at the tricritical point^{8,13}). Heat capacity measurements by Brisbin et al.¹⁴ on $\bar{n}S5$ series showed that for $\bar{8}S5, r = 0.936; a = 0$; for $\bar{9}S5, r = 0.96; a = 0.22$; and for $\bar{10}S5, r = 0.985; a = 0.45$. They made the important observation that $\bar{n}S5$ homologous series reveal the presence of critical-tricritical crossover behaviour upon increasing the chain length which in turn reduces the nematic phase temperature range. Heat capacity measurements of Thoen et al¹⁵ on nCB materials also showed a similar behaviour. α which had a value of -0.03 (in a mixture of 7CB and 8CB), increases with increase in r , having $\alpha=0.32$ for 8CB ($r=0.978$) and approaches a tricritical value of 0.5 with further increase in

r ($=0.994$ for 9CB). Similar crossover behaviour in α is seen in other systems also.¹⁶⁻¹⁸ The value of r for which tricritical behaviour is observed is equal to ~ 0.994 in 9CB-10CB system,¹⁵ $r \sim 0.984$ for nS5 series^{14,19} and $r \sim 0.992$ in 8CB-10CB system.¹⁶ This value of r showing a tricritical behaviour is much larger than the theoretically predicted value of 0.87 .² This also suggests that in order to see a first order Sm A-N transition, systems with a very narrow nematic range should be studied.

The measurement of density is a fundamental property in understanding phase behaviour. In particular, the continuity or discontinuity of the transition can be confirmed by precise measurements of density as a function of temperature. But there are only few such investigations.²⁰⁻²² The reason could be that even across the first order Sm A-N transition the density changes are expected to be quite small which would call for high precision measurements. In this chapter we present precise density measurements near the Sm A-N transition in materials with a very narrow nematic temperature ranges.

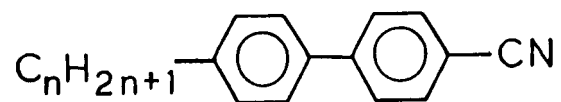
5.2 Experimental

5.2.1 Materials Used

Experiments were conducted on 4-n-nonyl-4'-cyanobiphenyl or 9CB and binary mixtures of it with its higher homologue 10CB.²³ The structural formulae and transition temperatures of these compounds are given in Table 5.1.

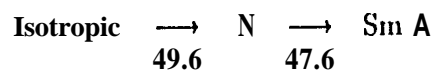
Density studies near Sm A-N tricritical point

nCB



4'-n-alkyl-4-cyanobiphenyl

9CB



10CB

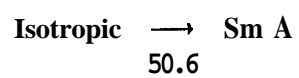


Table 5.1: Structural formulae and transition temperatures (in °C) of 9CB & 10CB.

Density studies near Sm A-N tricritical point

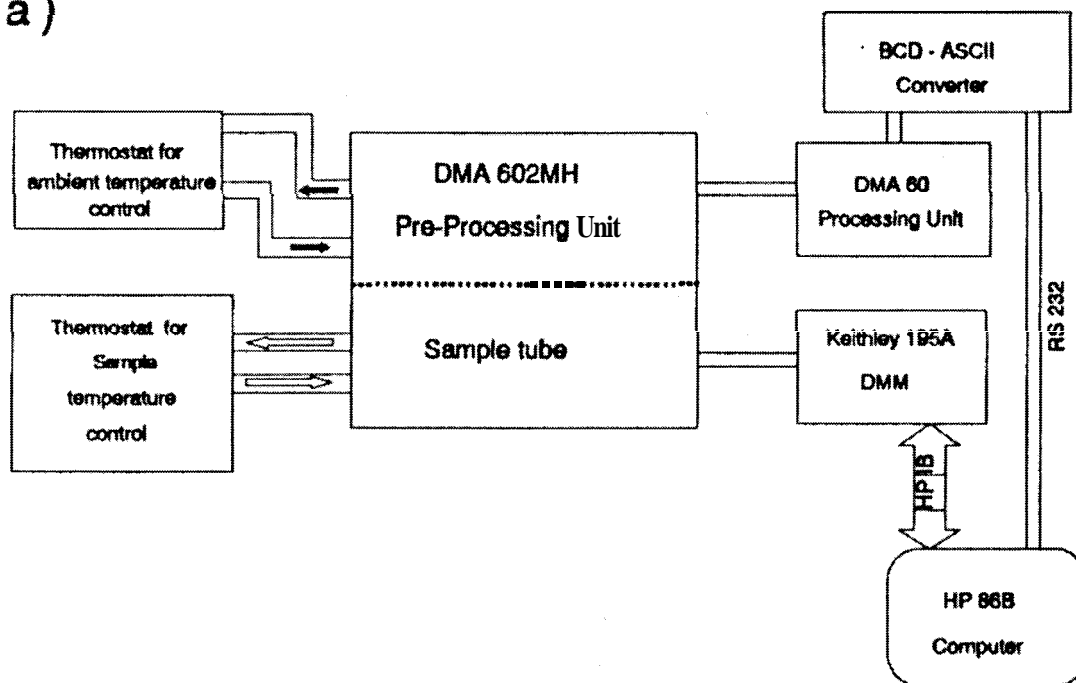
5.2.2 Density Measurement

Density measurements were made using an Anton Paar instrument consisting of a microcell (DMA 602MH) and a digital processing unit (DMA60). A block diagram of the experimental setup is shown in figure 5.1. The principle of determining density involves measuring the period of oscillation of a glass tuning fork filled with the sample to be studied.

The microcell consists of a hollow oscillator made out of borosilicate glass (Duran 50) fused into a dual wall glass cylinder. The space between the U-shaped sample tube and the inner wall of the dual wall cylinder is filled with a gas of high thermal conductivity. This will facilitate a rapid temperature equilibration of the sample with the thermostat liquid. The microcell has been provided with ports which can be connected to a bath liquid circulator. A high flash point low viscosity (Thermal H, Julabo) was circulated around the microcell using silicon tubings. The temperature of this liquid was varied and controlled by a precision thermostat (Hetofrig CB7). For good thermal regulation the length of the tubes between the thermostat and the density meter were kept as short as possible and were well insulated. A high precision potentiometer placed in conjunction with the preset on the thermostat control, made it possible to achieve long term stability of the sample temperature to better than 10mK. Although the electronic pre-processing unit on DMA602MH (which initiates and maintains the sample tube oscillations) is thermally insulated from the sample chamber, to achieve better signal to noise ratio, the processing part was maintained at room temperature by circulating water with the help of another circulator (Julabo

Density studies near S_m A-N tricritical point

(a)



(b)



Figure 5.1: (a) Block diagram of the experimental setup. (b) Sample cell.

water circulator).

The actual temperature of the sample was measured using a high resistance ($1\text{ M}\Omega$ at 25°C) and a large temperature coefficient bead thermistor (YSI 44011). It was inserted in a short capillary tube provided inside the inner space of the dual wall cylinder thereby ensuring determination of the true sample temperature. The resistance of the thermistor was measured using a four probe configuration by a digital multimeter (Keithley 195A). For the purpose of obtaining a numerical conversion between the resistance R of the thermistor and the measured temperature T ($^\circ\text{C}$), the table of R and T ($^\circ\text{C}$) values supplied by the manufacturer were fitted to the following expression.²⁴ [As a second check we also measured the resistance as a function of temperature by placing the thermistor in a calibrated programmable hot stage (Mettler FP 82). The measured and tabulated values were found to be in excellent agreement over the entire range of interest, viz., $25\text{-}100^\circ\text{C}$].

$$T = \frac{1}{C_0 + C_1 \times A + C_2 \times A^2 + C_3 \times A^3} - 273.15 \quad (5.2)$$

Here $A = \log(R)$. T is the calculated value of temperature in $^\circ\text{C}$. Figure 5.2 shows the fit of the data to the above expression.

As mentioned earlier, the underlying principle is the determination of the change in the natural frequency of vibration of a hollow oscillator when the density of the filled fluid changes. The oscillator tube is electronically excited in an undamped harmonic fashion. The direction of oscillation is perpendicular to the plane of the U-shaped sample tube. The density ρ of the sample is given by

$$\rho = K(\tau^2 - C) \quad (5.3)$$

Density studies near Sm A-N *tricritical* point

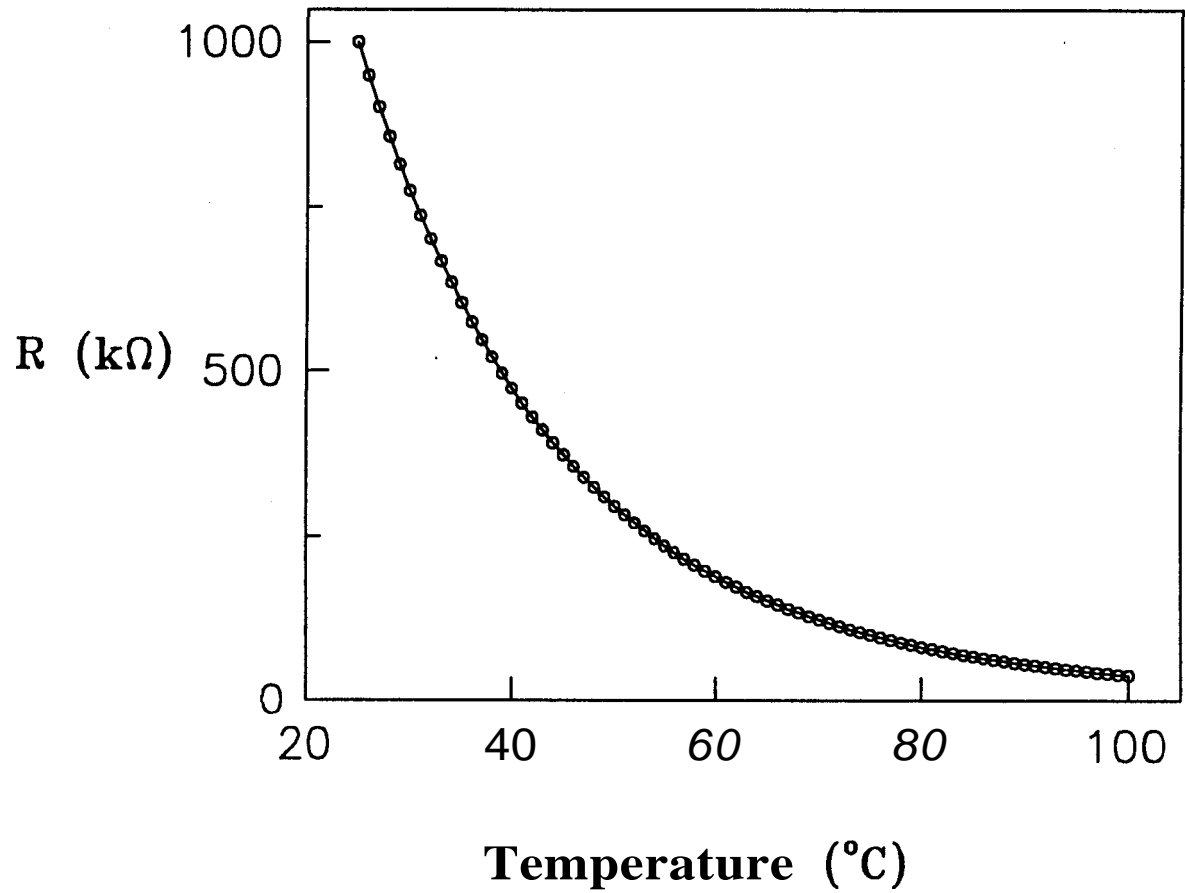


Figure 5.2: Plot of calibration curve of the thermistor. Solid line is a fitting to equation 5.2.

where, τ is the period of oscillation. Owing to the properties of the glass used the constants K and C are temperature dependent. These instrument constants were determined by measuring τ values for two samples with known density values. For this purpose we used air and water. A brief description of this calibration procedure is given below.

Calibration of the Instrument

The sample chamber was thoroughly cleaned to avoid traces of any foreign particles. The tube was set into oscillation and the period τ_{air} was read on the processing unit. The τ values were observed to be constant over long periods of time (> 2 hours), a further evidence of the absence of any foreign substances. For better statistics the period τ was measured over a large number of oscillations (10,000 cycles). In order to ensure that the scans taken for the liquid crystalline samples lie well within the calibration runs, the readings of τ_{air} were taken from 30-70°C at 1°C intervals. The second substance used was double-distilled water. To make sure that the filling of water is uniform the following procedure was adopted. Water was taken into a hypodermic syringe which had a specially made tip such that it fits snugly into the inlet port of the sample tube. Care was taken to see that the introduction of water takes place slowly, the meniscus of the water filling the tube should be concave and not convex. This is to avoid trapping micro air bubbles on the wall of the sample tube which prevents stable period readings. After filling the sample tube with water the two openings of the microcell were closed with a teflon stopper. τ_{water} as a function of temperature is measured in a similar way as for τ_{air} . The ratio of τ_{air} to τ_{water}

agreed with the values given by the manufacturer. The instrument constants K and C are calculated in the following manner.

$$\begin{aligned} \rho_{air} &= K(\tau_{air}^2 - C) \\ \rho_{water} &= K(\tau_{water}^2 - C) \end{aligned} \quad (5.4)$$

The values of ρ_{air}, ρ_{water} were taken from Handbook of chemistry and physics, 60th edition, CRC Press 1979. K and C were calculated using

$$\begin{aligned} K &= \frac{\rho_{air} - \rho_{water}}{(\tau_{air}^2 - \tau_{water}^2)} \\ C &= (\tau_{air}^2 - \frac{\rho_{air}}{K}) \end{aligned} \quad (5.5)$$

The values of K and C were determined at each temperature of these calibration scans. Figure 5.3 shows a plot of K and C versus temperature. For mathematical convenience they were fitted to a straight line with temperature as the independent variable. Using these constants, K and C the density of sample can be determined by measuring the period τ at any given temperature.

Before filling the liquid crystalline sample the sample tube was cleaned with alcohol and flushed using a built-in air pump. This procedure was repeated until the displayed τ values coincided with that of τ_{air} measured during the calibration process. Since the higher viscosity of the smectic A phase may preclude uniform filling, the samples were filled in the nematic phase. For all the materials studied, the Sm A-N transition is above room temperature. Hence the syringe had to be heated for the filling operation. A cylindrical copper heater surrounding the syringe was used for this purpose. The sample thus preheated to be in

Density studies near Sm A-N tricritical point

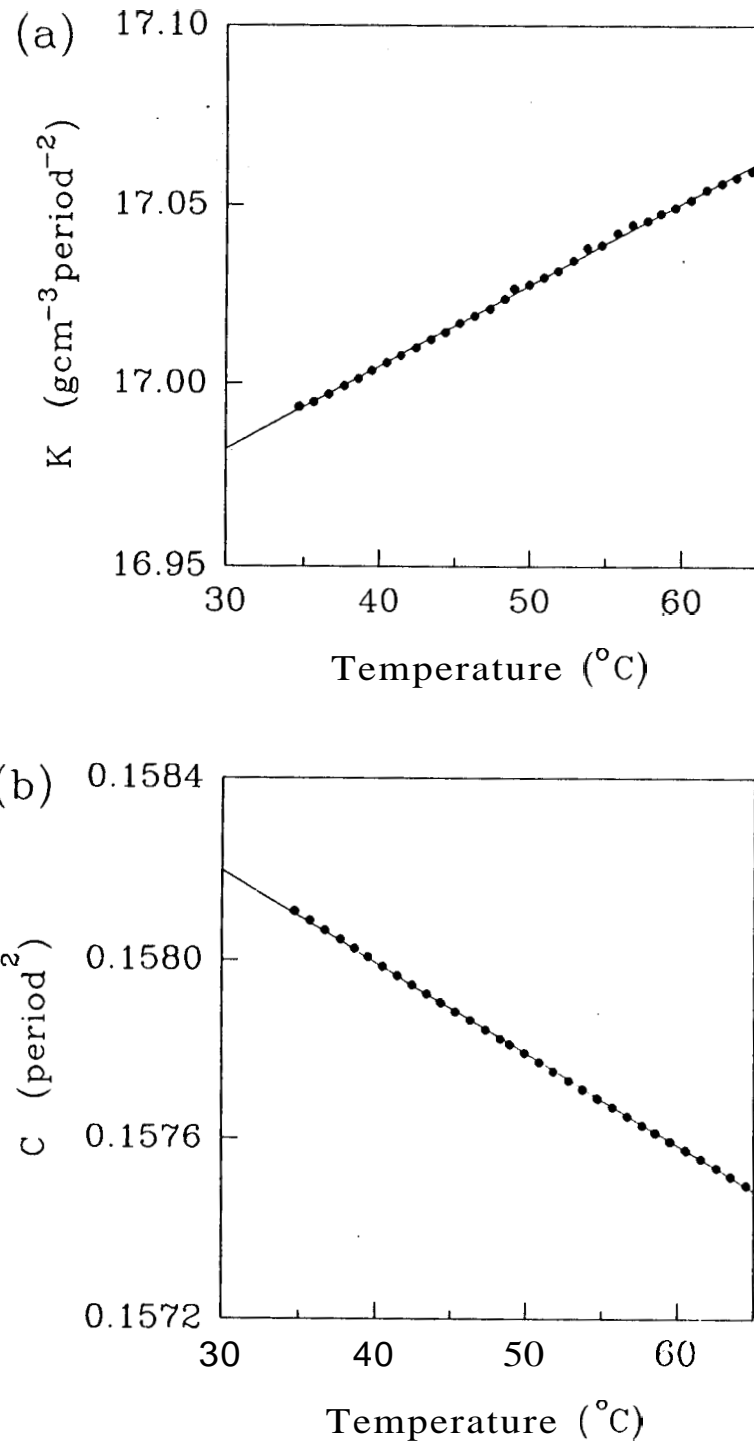


Figure 5.3: (a) Temperature variation of constant K and (b) constant C . Solid line is a fitting to a straight line.

the nematic phase was injected carefully into the oscillator (which is also kept above the *Sm A-N* transition temperature) in such a way that there were no air bubbles. The sample was cooled slowly to be well in the smectic A phase before starting the run. Now the temperature of the sample was varied with a step size dependent on the proximity to the transition. Between two temperature intervals, sufficient time (~ 10 minutes) was given for the thermal stabilisation of the sample. The equilibration of the temperature at any set point was monitored till it was constant to within 10mK . For better statistics, at each temperature τ value was recorded for 5 different cycles. DMA60 has a BCD output. For ease of interface this was converted to ASCII format using a home made BCD-ASCII converter which in turn was interfaced to HP 86B computer through an RS232 port. The temperature measuring multimeter (Keithley 195A) was also interfaced to HP 86B. The precision in the determination of density is $5 \times 10^{-5} \text{g/cm}^3$. The off-line analysis of the data has been carried out using a PC 386 personal computer.

5.3 Results and Discussion

9CB exhibits isotropic \rightarrow N \rightarrow Sm A as the phase sequence with decrease in temperature whereas 10CB shows a direct isotropic \rightarrow Sm A phase transition. The partial temperature-concentration (T-X, where X is the mole fraction of 10CB in the mixture) phase diagram of the 10CB-9CB system obtained using optical observations is shown in figure 5.4. The temperature range of the nematic phase which is already small for the 9CB (2°C) further decreases on addition of 10CB and finally ceases to exist for concentrations, $X > 0.35$.

Density studies near Sm A-N *tricritical* point

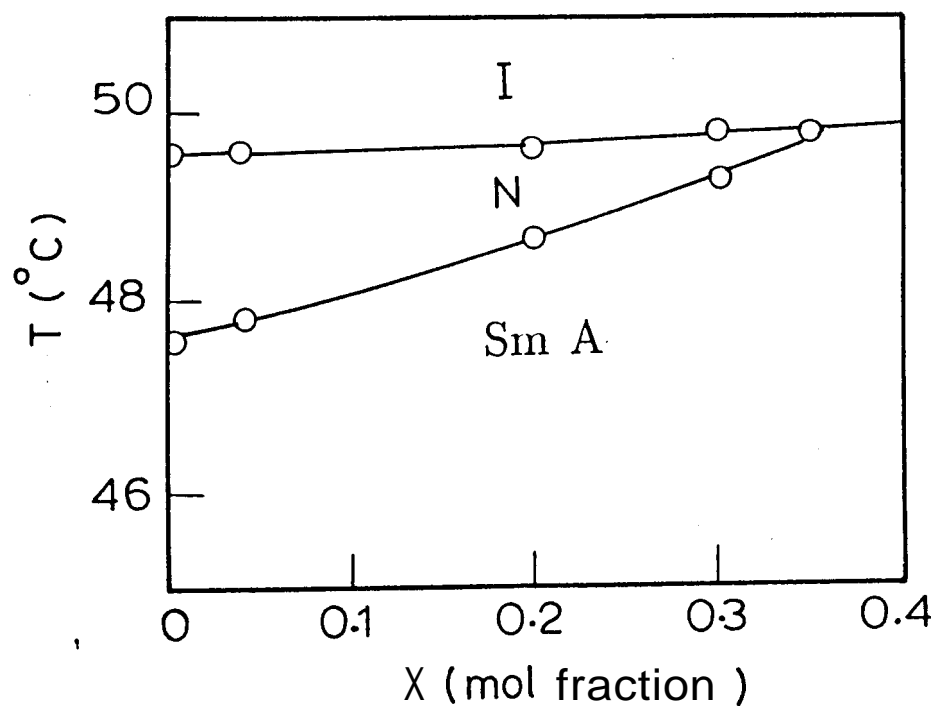


Figure 5.4: Part of the temperature-concentration phase diagram of 10CB-9CB system. X is the mole fraction of 10CB in the mixture.

Density experiments have been carried out on 9CB and for three mixtures of 10CB with 9CB, viz., for $X=0.04$, 0.2 and 0.3. Figure 5.5 is a representative plot showing the thermal variation of density near the Sm A-N and N-isotropic transition. From this plot it can be seen that the thermal variation of density has an abrupt change across the transition, whereas it shows smoother variation within the phase. The value of density, ρ changes by $\simeq 0.54\%$ across N-isotropic transition but only by $\simeq 0.2\%$ near N-Sm A transition. These features are in very good agreement with the earlier studies of Dunmur et al.,²⁰ on nCB series. The decrease in density values on going from smectic A to nematic and a much lower value in the isotropic phase reflects the decrease in the degree of molecular order in these phases. Similar behaviour is seen for 9CB and $X=0.2$ and 0.3 mixtures.

Although the thermal variation of density (ρ) across Sm A-N transition shows a concentration dependence, it was not significant enough to locate the tricritical point accurately. Zywocinski et al.^{21,25} pointed out that the asymptotic variation of thermal expansion near the phase transition can be described by a simple power-law equation with the exponent being equal to $(1-a)$ where a is the heat capacity exponent. Hence the density variation has been fitted to a simple power law^{16,19,26} of the form

$$|\delta\rho| = |\rho - \rho_o| = A_{\pm}|t|^{1-\alpha} \quad (5.6)$$

where $t = \frac{T-T_{AN}}{T_{AN}}$, T_{AN} denotes the Sm A-N transition temperature, ρ_o is the value of ρ at T_{AN} . Figure 5.6 is a representative plot of the density variation in the vicinity of T_{AN} . Also shown is the fit to equation 5.6. It is observed that

Density studies near Sm A-N tricritical point

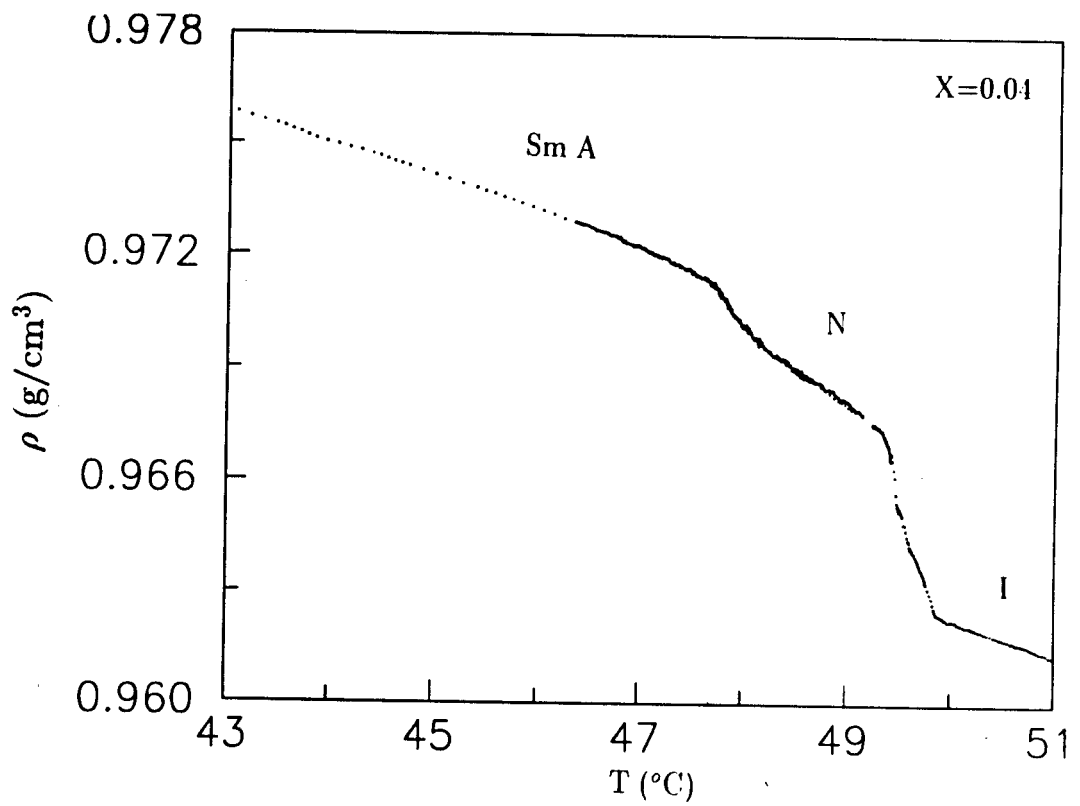


Figure 5.5: The temperature variation of the density (ρ) in the smectic A, nematic and isotropic phases for $X=0.04$.

Density studies near Sm A-N tricritical point

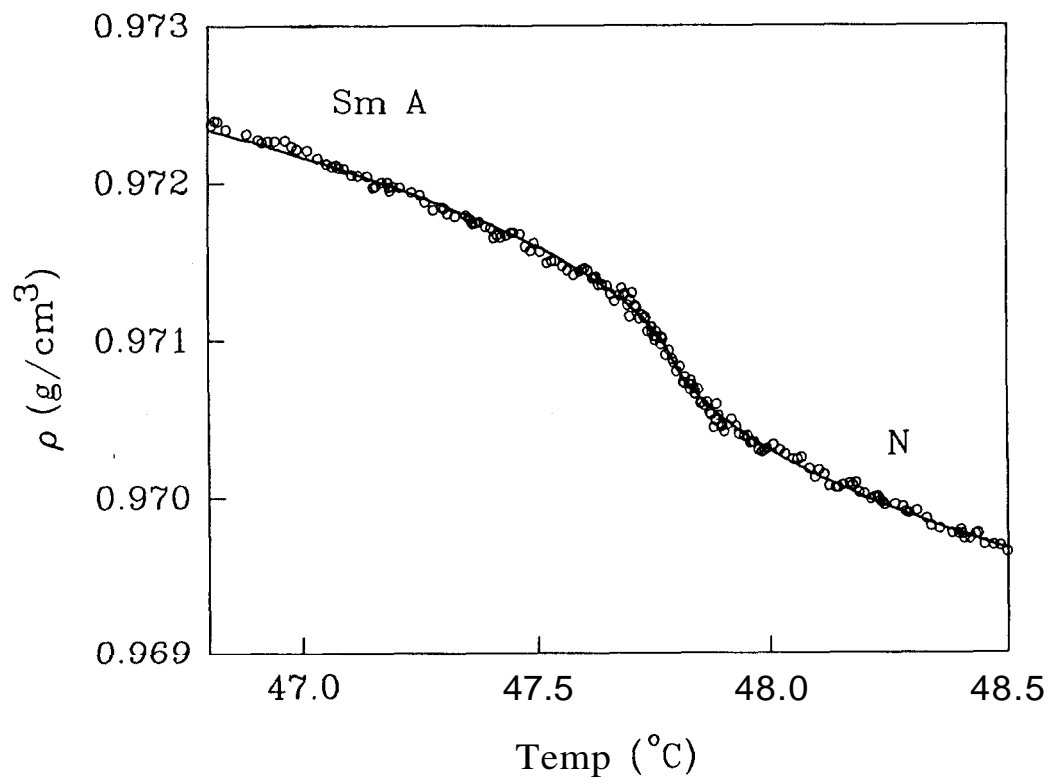


Figure 5.6: Thermal variation of ρ for $X=0.04$. Solid line is a fitting to a simple power. (Equation 5.6).

the simple power law is sufficient to describe the data. A simple way of checking this fitting would be to plot the data on a double logarithmic scale (i.e., $\log|\delta\rho|$ versus $\log t$). A plot of $\log|\delta\rho|$ versus $\log t$ would be a straight line with the slope being equal to $(1 - \alpha)$. Figures 5.7 and 5.8 show such plots for $X=0.04$ and 0.2 respectively. Some observations that can be made by looking at these fits are

1. The data above and below the transition show the same asymptotic behaviour, i.e., they are described by the same exponent.
2. For both 9CB & $X=0.04$, the powerlaw description holds good, indicated by the data falling on a straight line, suggesting that the transition is second order in nature. The values of the exponent are $\alpha = 0.5 \pm 0.01$ for $X=0.04$ with a smaller nematic range; $T_{NI}-T_{AN} = 1.7^\circ C$ and $r=0.995$ whereas $\alpha = 0.43 \pm 0.01$ for 9CB, with $T_{NI}-T_{AN} = 2^\circ C$; $r=0.994$. In contrast the data for $X=0.2$ shows a clear deviation from the linear behaviour—evidently a signature of a first order transition.^{19,27} Similar behaviour was observed for $X=0.3$ mixture also.

Thus the N-Sm A transition is first order for $X=0.2$ and is second order for 9CB. Recall that at a tricritical point $\alpha=0.5$. Since the $X=0.04$ mixture shows a value exactly equal to 0.5, we conclude that this mixture should be at or in the immediate vicinity of a tricritical point.

To check the reliability of these results a temperature dependent linear

Density studies near Sm A-N tricritical point

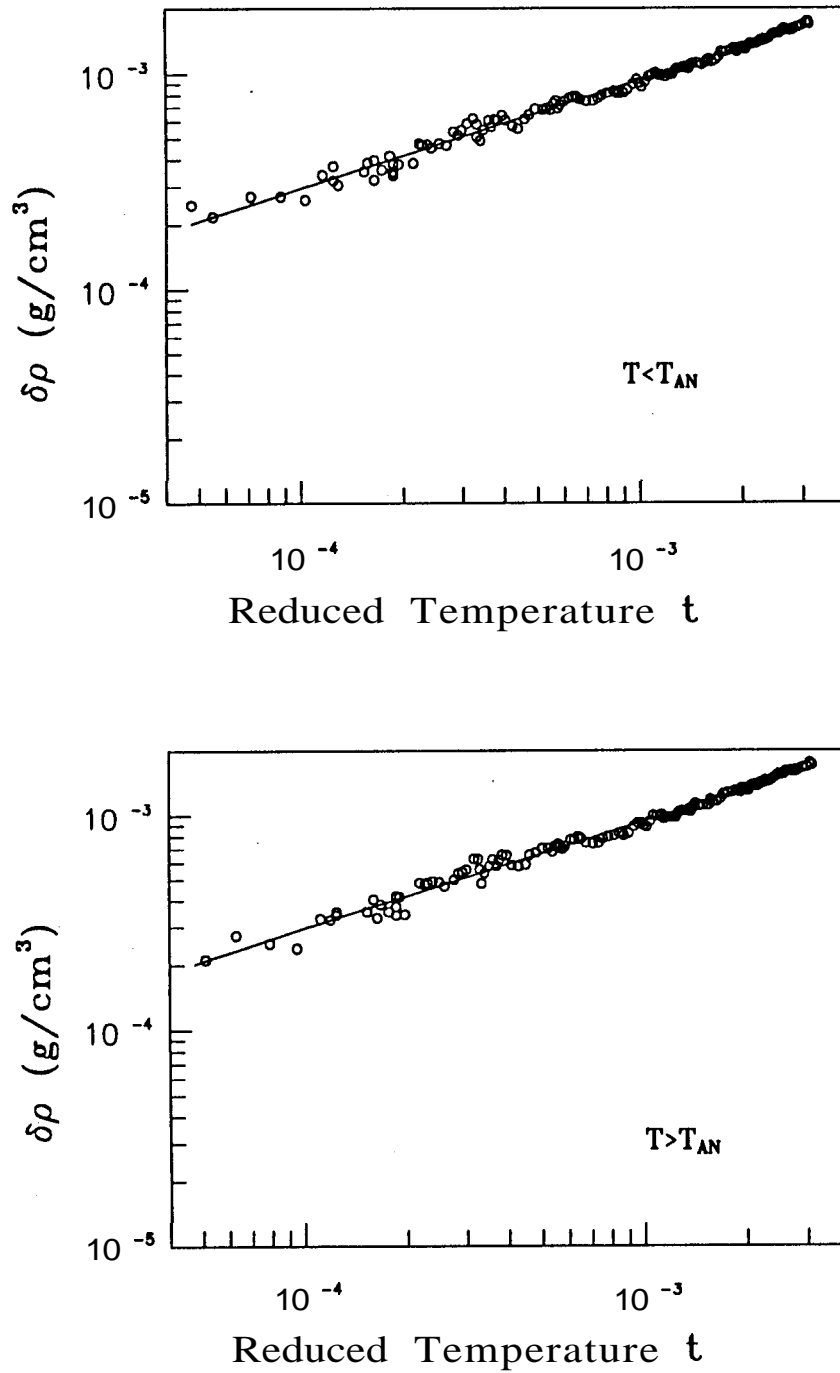


Figure 5.7: Double logarithmic plots for $X=0.04$. Solid line is a fitting to equation 5.6. Goodness of the fitting even very close to the transition ($t = 5 \times 10^{-5}$) indicates the second order nature.

Density studies near *Sm* A-N tricritical point

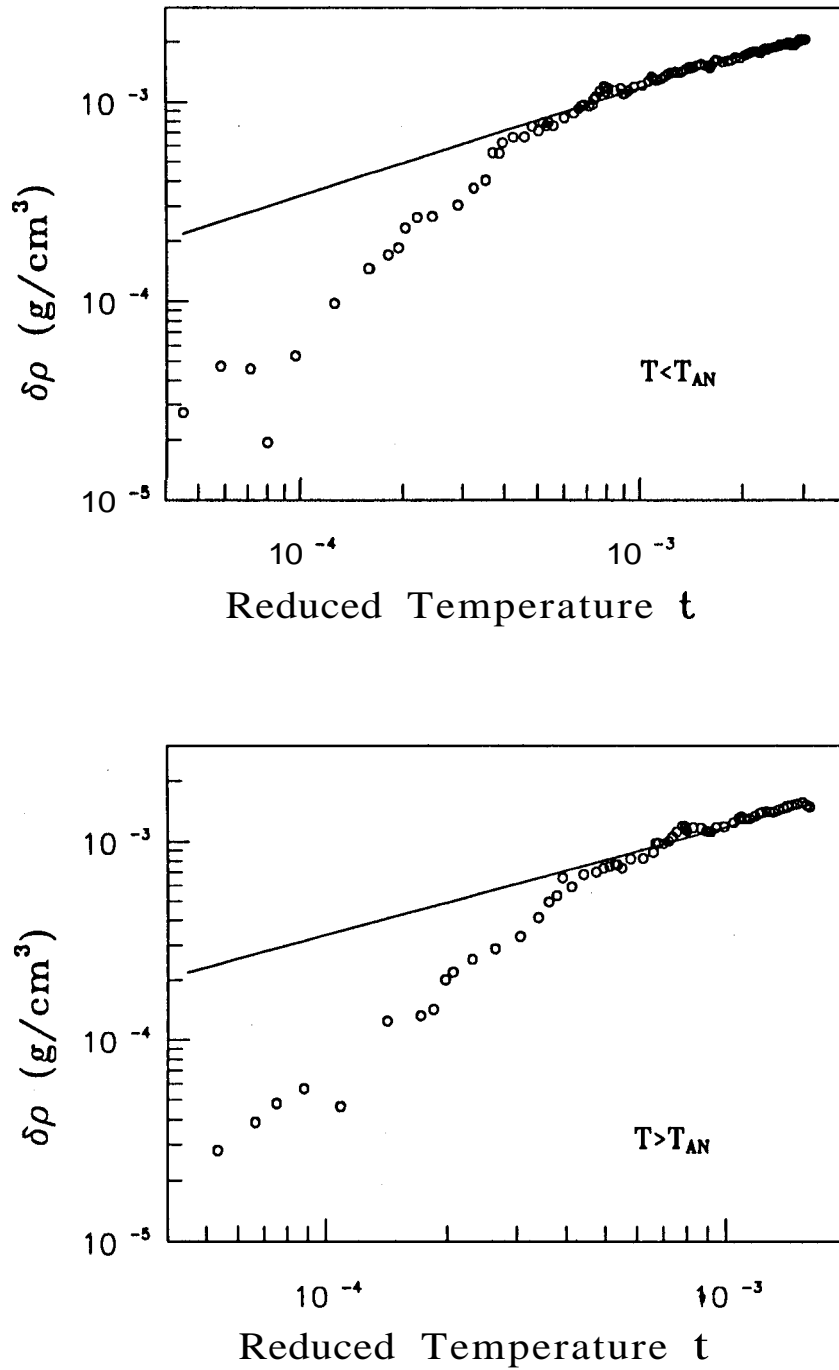


Figure 5.8: Double logarithmic plots for $X=0.2$. Solid line is a fitting to equation 5.6. Deviation of the data from the straight line suggests the first order nature of the transition.

Density studies near Sm A-N tricritical point

background term was added to the powerlaw expression (equation 5.7).

$$|\delta\rho| = A_{\pm}|t|^{1-\alpha} + B|t| \quad (5.7)$$

where, B is a constant. Results of computations carried out using equation 5.7 do not change the conclusions arrived using the simple powerlaw form (the contribution due to the linear term is observed to be less than a few percent far away from the transition decreasing as the transition is approached).

It may be mentioned that Thoen et al.¹⁵ have measured latent heat (AH) using adiabatic calorimetric technique in the mixtures of 9CB and 10CB. Figure 5.9 shows a plot of AH vs temperature near Sm A-N transition in 9CB and mixtures of 9CB+10CB. AH which is highest for the largest 10CB mole fraction, decreases drastically with decrease in X or with an increase in nematic range. From an extrapolation of AH versus r curve to zero they showed that the *tricritical* point is located very close to pure 9CB with $r=0.994$ (see figure 5.9). Ocko et al.¹⁹ have measured longitudinal and transverse correlation lengths ($\xi_{\parallel}, \xi_{\perp}$) near the N-Sm A transition using high resolution X-ray scattering techniques in the same system (see figures 5.10 and 5.11). The temperature dependence of ξ_{\parallel} and ξ_{\perp} could be described by a single powerlaw (see figures 5.10 and 5.11). Further, their results also indicated the tricritical point to lie at or very close to $X=0.09$. Thus our density measurements are in very good agreement with the calorimetric¹⁵ and X-ray results.¹⁹

In conclusion, we have carried out the first detailed density studies near Sm A-N tricritical point in 9CB-10CB mixtures. The results confirm the existence of a tricritical point for a concentration very near to $X=0.04$ mixture, in good agreement with earlier results.

Density studies near Sm A-N tricritical point

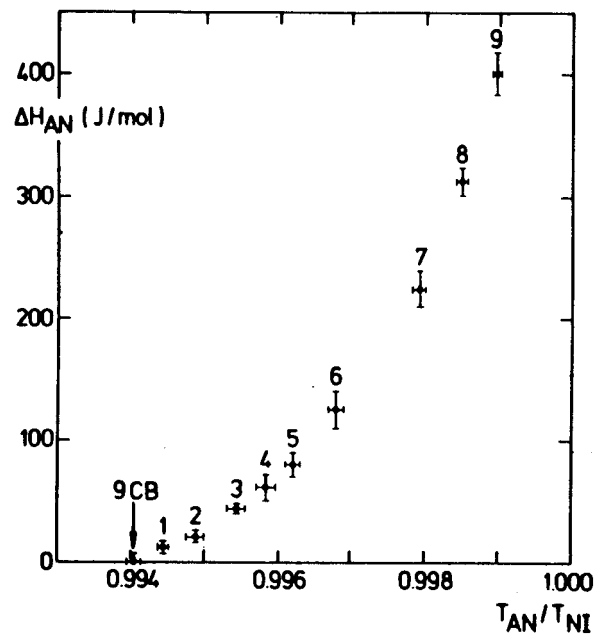


Figure 5.9: The Sm A-N latent heat ΔH_{AN} as a function of T_{AN}/T_{NI} for the 9CB-10CB mixtures. (From Ref. 15).

Density studies near Sm A-N tricritical point

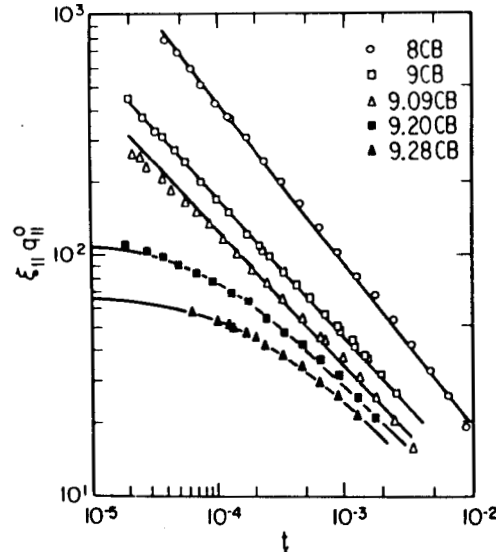


Figure 5.10: Longitudinal correlation length (ξ_{\parallel}) vs. reduced temperature (t) for **nCB** samples. The solid lines are single power law fits. For first order transitions ($X=0.2$ and 0.28) the behaviour is non-linear. Suitable corrections is applied by the authors for these concentrations. (From Ref. 19).

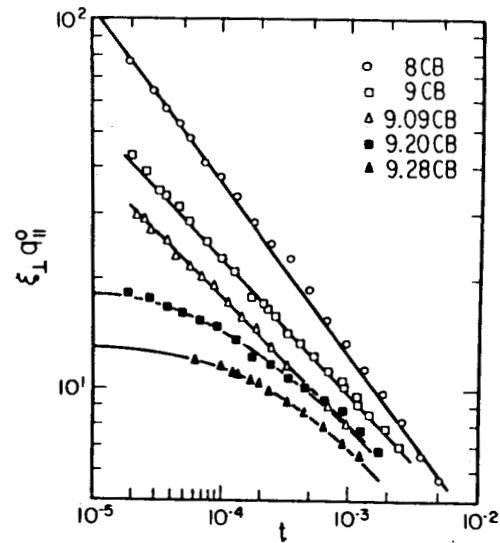


Figure 5.11: Transverse correlation length vs. reduced temperature (t) for **nCB** samples. The solid lines are single power law fits. For first order transitions ($X=0.2$ and 0.28) the behaviour is non-linear. Suitable corrections is applied by the authors for these concentrations. (From Ref. 19).

References

- [1] R.J.Birgeneau, C.W.Garland, G.B.Kasting and B.M.Ocko, *Phys.Rev. A* 24, 2624 (1981); C.W.Garland, M. Miechle, B. M. Ocko, A.R.Kortan, C.R.Safinya, L. J. Yu, J. D. Litster and R.J.Birgeneau, *Phys.Rev. A* 27, 3234 (1983).
- [2] W.L.McMillan, *Phys.Rev. A* 4, 1238 (1971).
- [3] P.G.de Gennes, *Solid State Commun.* 10, 753 (1972).
- [4] B.I.Halperin, T.C.Lubensky and S.K.Ma, *Phys.Rev.Lett.*, 32, 292 (1974); W.Helfrich, *J.Phys.(Paris)*, 39, 1199 (1978); Nelson and J.Toner, *Phys.Rev. B* 24,363 (1981); T.C.Lubensky, S.C.Dunn and J.Isaacson, *Phys.Rev.Lett.*, 22, 1609 (1981); T.C.Lubensky, *J.Chim.Phys* 80, 31 (1983).
- [5] C.Dasgupta, *J.Phys. (France)*, 48, 957 (1987).
- [6] C.Dasgupta and B.I.Halperin, *Phys.Rev.Lett.*, 47, 1556 (1981).
- [7] J.Toner, *Phys.Rev. B* 26, 402 (1982).
- [8] The current situation regarding theoretical and experimental studies on N-Sm A transition has been summarised in S.Chandrasekhar, Chapter 5, *Liquid Crystals*, Cambridge University Press, 1992.
- [9] C.Bagnauls and C.Bervillier, *Phys.Rev. B* 32, 7209 (1985).
- [10] K.K.Chan, M.Deutsch, B.M.Ocko, P.S.Pershan and L.B.Sorensen, *Phys.Rev.Lett.*, 54, 920 (1985); Evans-Lutterodt, J.W.Chung, B.M.Ocko,

- R.J.Birgeneau, C.Chang, C.W.Garland, E.Chin, J.Goodby and N.H.Tinh, *Phys.Rev. A* 36, 1387 (1987); G.Nounesis, M.J.Young, K.I.Blum, C.W.Garland and R.J.Birgeneau, *Z.Phys.B (Condensed Matter)*, 90, 357 (1993); B.M.Ocko, R.J.Birgeneau, J.D.Litster and M.E.Neubert, *Phys.Rev.Lett.*, 52,208 (1984); R.Mahmood, D.Brisbin, I.Khan, C.Gooden, A.Baldwin, D.L.Johnson and M.E.Neubert, *Phys.Rev.Lett.*, 54, 1031, (1985); S.Sprunt, L.Solomon and J.D.Litster, *Phys.Rev.Lett.*, 53, 1923, (1984); M.Benzekro, J.D.Marcerou, H.T.Nguyen and J.C.Rouillon, *Phys.Rev. B* 41, 9032 (1990).
- [11] C.W.Garland, G.Nounesis, K.J.Stine and G.Heppke, *J.Phys. (France)*, 50, 2291 (1989).
- [12] W.G.Bouman and W.H.de Jeu, *Phys.Rev.Lett.*, 68, 800 (1992).
- [13] M.Plischke and B.Bergersen, *Equilibrium Statistical Physics*, Prentice Hall Advanced Reference Series, 1989.
- [14] D.Brisbin, R.DeHoff, T.E.Lockhart and D.L.Johnson, *Phys.Rev.Lett.*, 43, 1171 (1979).
- [15] J.Thoen, H.Marynissen and W.Van Dael, *Phys.Rev.Lett.*, 52, 204 (1984).
- [16] H.Marynissen, J.Thoen and W.Van Dael, *Mol.Cryst.Liq.Cryst.*, 124, 195 (1985).
- [17] K. J. Stine and C. W. Garland, *Phys. Rev.* **A39**, 3148 (1988); M. E. Huster, K. J. Stine and C. W. Garland, *Phys. Rev.* **A36**, 2364 (1987);

- M. A. Anisimov, V. P. Voronov, A. O. Kulkov, V. N. Petuknov and F. Kholmurodov, *Mol. Cryst. Liq. Cyst.*, **150**, 399 (1987).
- [18] H.Marynissen, J.Thoen and W.Van Dael, *Mol.Cyst.Liq.Cryst.*, **97**, 149 (1983).
- [19] B.M.Ocko, R.J.Birgeneau and J.D.Litster, *Z.Phys.* **B62**, 487(1986).
- [20] D.A.Dunmur and W.H.Miller, *J.Phys. Coll.*, *C3* 40, 141 (1979).
- [21] A.Zywocinski, S.A.Wieczorek and J.Stecki, *Phys.Rev.* **A36**, 1901 (1987).
- [22] S.Torza and P.E.Cladis, *Phys. Rev. Lett.*, **32**, 1406 (1974); A.J.Leadbetter, J.L.A.Durrant and M.Rugman, *Mol.Cryst.Liq.Cryst.Lett.*, **34**, 231 (1977); M.F.Achard, F.Hardouin, G.Sigaud and M.Mauzac, *Liquid Crystals*, **1**, 203 (1986).
- [23] 9CB and 10CB are kindly given to us by BDH(Poole) Ltd.
- [24] B.W.Magnum, *Rev.Sci.Instrum.*, **54**, 1687 (1983).
- [25] A.Zywocinski, S.A.Wieczorek, *Phys.Rev. A* **31**, 479 (1985).
- [26] C.Rosenblatt and J.T.Ho, *Phys.Rev. A* **26**, 2293 (1982); C.W.Garland, G.B.Kasting and K.J.Lushington, *Phys.Rev.Lett.* **43**, 1420 (1979); T.Pitchford, G.Nounesis, S.Dumrongrattana, J.M.Viner, C.C.Huang and J.W.Goodby *Phys.Rev. A* **32**, 1938 (1985).
- [27] K.K.Chan, P.S.Pershan, L.B.Sorensen and F.Hardouin, *Phys.Rev.Lett.*, **54**, 1694 (1985).